Chapter 3

The Ingredients-Based Methodology for Forecasting Winter Season Precipitation Events

The IBM for forecasting winter season precipitation events was introduced in Chapter 1, and the five key ingredients were identified to be QG forcing for vertical motion, moisture, instability, precipitation efficiency, and temperature. Instability was investigated in Chapter 2, including an analysis of the mechanisms that govern the evolution of instabilities in mid-latitude cyclones. In Chapter 3, the five ingredients are formally described and the diagnostics used to quantify their contributions are introduced. The application of the IBM to forecasting winter precipitation is also discussed, and a case study of a strong midwestern snow storm is presented.

3.1 Ingredient Descriptions

3.1.1 Forcing for Ascent

As an initially unsaturated column of air is lifted by some forcing mechanism, its temperature decreases until saturation occurs. Provided sufficient condensation or ice nuclei are present, any additional lifting after saturation is achieved results in the condensation of water vapor to liquid or ice, which can eventually fall out as precipitation. This section addresses the forcing ingredient and presents a diagnostic for quantifying the degree of quasi-geostrophic (QG) forcing.

Most traditional forecast techniques for the prediction of winter season precipitation do not specifically consider forcing for ascent. The Magic Chart (Sangster and Jagler, 1985; Chaston, 1989) is the only technique listed in Table 1.1 that directly includes vertical motion in its forecast algorithm. Instead of considering forcing for ascent, however, the Magic Chart uses the net vertical displacement (NVD) of air parcels reaching the 700 hPa level at the end of the 12-hour forecast period (Reap, 1990). The Garcia Method (Garcia, 1994) does not include forcing for ascent directly, however it explicitly states that the "area of concern" chosen by the forecaster must coincide with some forcing mechanism before the technique can be applied. Since it already prescribes an independent analysis of the forcing ingredient, the Garcia Method (Garcia, 1994) can be integrated nicely into the IBM, as will be shown later.

With modern tools available for the analysis of gridded data, it is not difficult to compute diagnostics of QG forcing for vertical motion. One such diagnostic uses the

Q-vector form of the adiabatic and inviscid QG-ω equation (Hoskins et al., 1978):

$$\left(\sigma\nabla^2 + f^2\frac{\partial^2}{\partial p^2}\right)\omega = -2\nabla\cdot\vec{Q} \tag{3.1}$$

where

$$\vec{Q} = \left[-\frac{\partial\vec{V}_g}{\partial x}\cdot\left(-\frac{\partial\phi}{\partial p}\right)\hat{\imath}, -\frac{\partial\vec{V}_g}{\partial y}\cdot\left(-\frac{\partial\phi}{\partial p}\right)\hat{\jmath}\right]$$

and

$$\omega = \frac{dp}{dt}$$

and the variables are used as defined in Chapter 2. As discussed in Chapter 2, the left-hand side is similar to a 3-D Laplacian, except that this pseudo-Laplacian operator is modulated by a stability parameter σ and the Coriolis parameter f. A formal solution of equation 3.1 would require a distribution of $\vec{Q}$ in an isobaric layer and boundary conditions for ω.

Often a qualitative estimate of forcing for vertical motion is all that is necessary in an operational environment. Recognizing that the forcing $\nabla\cdot\vec{Q}$ and the response ω are related by the pseudo-Laplacian operator, equation 3.1 provides a means of making a qualitative estimate. Convergence of the Q-vector ($\nabla\cdot\vec{Q} < 0$) corresponds to a negative ω and thus forcing for upward vertical motion. Divergence of the Q-vector ($\nabla\cdot\vec{Q} > 0$) corresponds to forcing for downward vertical motion. Thus, isobaric contours of $\nabla\cdot\vec{Q}$ computed at a number of levels, in conjunction with a cross-sectional analysis, provide a qualitative estimate of the direction and magnitude of the vertical motion forcing throughout the atmosphere.

Based on an evaluation of a number of case studies, a classification for describing the QG magnitude of forcing was developed and is shown in Table 3.1. These ranges are

$\nabla \cdot \vec{Q}$ $(Km^{-2}s^{-1}$ x $10^{-15})$	Classification
-1 to -5	Weak Forcing
-5 to -15	Moderate Forcing
$<$ -15	Strong Forcing

Table 3.1: Classification of Q-vector forcing.

intended to provide a consistent terminology for discussing the strength of QG forcing for ascent. Provided that the atmosphere is well-described by the QG equations (i. e., low Rossby number flow), there is ample moisture throughout the lower- to mid-troposphere, and no instability, the categories in Table 3.1 roughly describe the intensity[1] of the ensuing precipitation. Weak forcing corresponds to light precipitation, moderate forcing to moderate precipitation, and strong forcing to heavy precipitation.

However, this approach to estimating the QG forcing for ascent neglects any modulation by the stability parameter, σ, because it involves approximating the pseudo-Laplacian operator $\left(\sigma\nabla^2 + f^2\frac{\partial^2}{\partial p^2}\right)$ with the true Laplacian. Since σ appears in the full form of the QG-ω equation (equation 3.1), accurate estimates of the magnitude of the upward vertical motions resulting from a given Q-vector convergence should include consideration of the atmospheric stability. Section 3.1.3 and chapter 2 will address the instability ingredient in more detail.

[1] Precipitation intensity is defined according to the system used for surface station observations: light precipitation corresponds to -SN or -RA (for snow or rain, respectively), moderate precipitation to SN or RA, and heavy precipitation to +SN or +RA.

It is important to remember that the use of the Q-vector diagnostic as a sole means for vertical motion forcing does impose limits on the analysis, namely, that it is only applicable in those regions where the Rossby number is low. No accommodation for the role of non-QG motions in modulating the observed vertical motions is made in the approach presented in this thesis. Such effects may be particularly significant in the vicinity of frontal zones or jet streaks. A useful addition to the present analysis would include a quantification of the degree to which each case agrees with its QG description.

3.1.2 Moisture

Given ample moisture, even very weak forcing can be sufficient to generate precipitation. However, precipitation will not be produced in a dry atmosphere even in the presence of strong forcing and instability. Thus, an evaluation of available moisture should be included in any forecast for precipitation.

There are a variety of ways to assess the moisture availability in a system. The Magic Chart (Sangster and Jagler, 1985; Chaston, 1989) leaves the evaluation of the moisture availability up to the forecaster, recommending an examination of the 500-1000 hPa layer-averaged relative humidity. The Garcia Method (Garcia, 1994) is based on the assumption that moisture is often the limiting factor in a snow event. It predicts a direct relationship between the mixing ratio on a mid-tropospheric isentropic surface and snowfall amounts. For a 12-hour period, in a region where snowfall is expected based on an evaluation of forcing mechanisms, the Garcia Method predicts that the maximum amount of snow (in inches) will equal twice the maximum mixing ratio (in g kg^{-1}) on an isentropic surface which intersects the 700-750 hPa layer over the forecast area. The Cook Method (Cook, 1980) draws from the theory of Jacobson et al. (1956) which holds that it isn't necessary to explicitly worry about moisture in a developing storm because if the dynamics are strong moisture will find its way into the storm.

The technique for evaluating moisture availability in this thesis first involves the inspection of relative humidity at a number of levels throughout the lower and mid-troposphere to determine the degree of saturation. Relative humidity is defined as the ratio of the actual mixing ratio (l) to the saturation mixing ratio with respect to water at the same temperature and pressure (l_s) and is typically expressed as a percent (Wallace and Hobbs, 1977):

$$RH = 100 \, \frac{l}{l_s} \tag{3.2}$$

After determining the degree of saturation, the available moisture must be quantified because relative humidity does not provide information about the absolute moisture content and, thus, cannot describe the amount or intensity of the resulting precipitation. For this purpose, we examine the mixing ratio l, defined as the ratio of the mass of water vapor (M_v) to the mass of dry air (M_d) in a parcel:

$$l = \frac{M_v}{M_d} \tag{3.3}$$

Mixing ratio was chosen for this technique because of our intent to integrate the ingredients technique with the Garcia Method for estimating snowfall accumulation. The Garcia Method is well suited for this purpose due to its comprehensive treatment of the moisture ingredient, including an analysis of mixing ratios on isentropic surfaces.

However, isentropic analysis is not appropriate for neutral or unstable conditions, nor regions where diabatic heating or cooling is occurring. This excludes any areas of instability and regions characterized by a phase change. By integrating the Garcia Method into the ingredients technique, situations when isentropic analysis cannot be accurately or prudently applied can be accommodated. This is discussed further in section 3.2.3.

3.1.3 Instability

In section 3.1.1, $\nabla \cdot Q$ was discussed as a technique for identifying regions of forcing for ascent. However, equation 3.1 reveals that an analysis of $\nabla \cdot Q$ alone will not account for the influence of atmospheric stability (σ) on the magnitude of the response (ω) to a forcing. Thus, in this thesis, the instability instability ingredient is considered whenever the Q-vector diagnostic is employed to account for the modulation of the response to a given forcing for ascent.

The stability parameter σ considers only gravitational instabilities and doesn't identify regions of symmetric instabilities. In order to allow for consideration of both types, we use saturated geostrophic equivalent potential vorticity, PV_{es_g}, in the IBM to diagnose the instability ingredient, where PV_{es_g} is defined by equation 2.5. By choosing to use PV_{es} rather than PV_e, only conditional gravitational (CI) and conditional symmetric instabilities (CSI) are considered, rather than potential gravitational (PI) and potential symmetric instabilities (PSI). Where PV_{es} is negative, CI exists if $-\frac{\partial \theta_{es}}{\partial p} < 0$ and CSI exists if $-\frac{\partial \theta_{es}}{\partial p} > 0$ and the atmosphere is characterized by two-dimensional flow. CI and CSI are measures of the susceptibility of the atmosphere to moist gravitational and moist symmetric convection, not indicators of the existence of such convection (SS). Thus, for either instability to be realized and convection to occur, saturation must be present locally and a mechanism to force an infinitesimal upward vertical motion must exist. It is important to distinguish between gravitational and symmetric instabilities only insofar as the atmosphere may respond differently, particularly with respect to the organization of precipitation bands in each type of instability. However, this distinction is not emphasized in the forecast technique presented in this thesis because both instability mechanisms have similar implications, namely increased snowfall amounts and the potential for lightning and thunder. Instead, the IBM will focus on identifying a region of instability, then leave it to forecasters to analyze cross-sections and decide if a vertical or slantwise response can be expected.

It would be useful to derive a relationship between $\nabla \cdot \vec{Q}$, PV_{es}, and ω to provide quantitative estimates of the vertical motion; however, this derivation is beyond the scope of this thesis. Instead, regions where enhanced vertical motions can be expected are identified based on the co-location of both forcing and instability. Since both negative $\nabla \cdot \vec{Q}$ (associated with upward vertical motion) and negative PV_{es} (associated with conditional instabilities) are indicative of a strong precipitation potential, regions with large positive values of the product $(\nabla \cdot \vec{Q})(PV_{es})$, computed where both terms are negative, have a strong likelihood for experiencing extreme precipitation events provided that sufficient moisture is available. Here, a new diagnostic parameter, QPV, is introduced to capture this effect. QPV is defined as

$$\begin{aligned} \text{QPV} &= \left(\nabla \cdot \vec{Q}\right)(PV_{es}) && \text{for negative } \nabla \cdot \vec{Q} \text{ and negative } PV_{es} \\ &= 0 && \text{for positive } \nabla \cdot \vec{Q} \text{ and/or positive } PV_{es} \end{aligned} \tag{3.4}$$

and computed as

$$QPV = \left(\frac{\nabla \cdot \vec{Q} - \left|\nabla \cdot \vec{Q}\right|}{2}\right)\left(\frac{PV_{es} - |PV_{es}|}{2}\right) \tag{3.5}$$

Where this positive product is large, there is forcing in the presence of instability, and strong upward vertical motion should be anticipated. Because the two quantities $\nabla \cdot \vec{Q}$ and PV_{es} span a different range of values, the absolute magnitude of the quantity QPV may be more sensitive to one than the other. Thus, we employ QPV as an indicator of the potential for convective precipitation without regard to its absolute magnitude. It is important to remember that PV_{es} need not be negative for precipitation to fall. In fact, heavy snow often results from strong forcing alone. Therefore, contours of QPV should only be used to identify areas of potentially convective snowfall. Many winter season precipitation events with sufficient forcing and moisture will be associated with positive PV_{es} and, thus, zero QPV.

3.1.4 Efficiency

Doswell et al. (1996) defined efficiency as the ratio of the mass of water falling as precipitation to the influx of water vapor mass into the cloud in their ingredients-based technique for forecasting precipitation associated with flash flooding, (see section 1.1). This ingredient served as their constant of proportionality in a relationship between rainfall rate, ascent rate, and mixing ratio. With knowledge of the processes governing the cloud microphysics, efficiency ingredient can be assessed in a more sophisticated manner. In this section the cloud microphysical processes that influence the efficiency of a winter precipitation event are discussed. First, the processes involved in the formation of ice from supercooled liquid droplets are examined. Then, the growth of ice particles following initiation, and the conditions that lead to maximum growth are discussed. Finally, ways to incorporate precipitation efficiency into the ingredients-based approach are identified.

Ice Nucleation

To initiate the precipitation process in cold clouds, supercooled liquid must freeze into an ice crystal. This can occur in three ways: heterogeneous nucleation, homogeneous nucleation, or deposition onto a pre-existing ice crystal. Heterogeneous nucleation is the process by which supercooled liquid condenses onto an ice nuclei to form an ice crystal. In homogeneous nucleation, supercooled liquid can form an ice crystal without any nuclei present, however this requires a temperature below -40^{o}C. Homogeneous nucleation is not considered here because it is not typically characteristic of winter storms at mid-latitudes. Furthermore,it is assumed that there are no ice crystals introduced into the layer of supercooled liquid, thus limiting the discussion to the initiation of ice crystals by heterogeneous nucleation.

The initiation of an ice crystal by heterogeneous nucleation requires a small particle, or nuclei. The ability of supercooled liquid to condense on the nuclei and form an ice crystal depends on the chemical makeup of the particle, and the temperature and relative humidity of the ambient air (Rogers and Yau, 1989). Over the upper Midwest, 80-90% of the ice nuclei (IN) are some form of clay, primarily vermiculite. Vermiculite requires an air temperature of -15^{o}C for ice nucleation to occur. Table 3.2 shows some typical IN and their corresponding activation temperatures. Because of the presence of

IN Composition	Activation Temperature
Silver Iodide	-4^{o}C
Kaolinite	-9^{o}C
Volcanic Ash	-13^{o}C
Vermiculite	-15^{o}C

Table 3.2: Examples of some typical ice nuclei (IN) and the temperature required for ice crystal activation on their surfaces, from Rogers and Yau (1989).

multiple types of IN in a cloud, and the variation of initiation temperature with ambient relative humidity and surface characteristics of the IN, a specific value cannot be assigned to the temperature at which ice nucleation is always initiated. Instead, guidelines determined by statistical studies must be used to identify a range of temperatures for which ice nucleation can be expected. Based on the results of a number of studies (e. g., Borovikov et al., 1963; Mossop et al., 1970), Baumgardt (1999) prepared guidelines for determining whether ice nuclei might be initiated within a cloud. These are shown in Table 3.3. Furthermore, Baumgardt (1999) concluded that -12^{o}C to -14^{o}C should be considered the minimum range for a good chance of ice being in a cloud, and offered

Cloud Temperature	Chance of Ice in the Cloud
$\leq -4^o$C	0% (No Ice)
-10^oC	60%
-12^oC	70%
-15^oC	90%
-20^oC	100%

Table 3.3: Guidelines for determining if ice nucleation has occurred in a cloud, adapted from Baumgardt (1999).

-10^oC as the operational cutoff point for no ice.

Ice Particle Growth

After initiation, ice particles can grow in the cloud through the following mechanisms, deposition, accretion, or aggregation. Growth by deposition involves the change from water vapor to ice when water vapor is deposited on ice or ice nuclei. This is governed by the Bergeron-Findeisen process in which ice crystals grow at the expense of liquid droplets in environments for which the relative humidity is 100%. Since the saturation vapor pressure over ice is less than that over water, the vapor is compelled toward the ice, depositing on the ice when it makes contact. The growth rate by deposition is greater at colder temperatures, with a maximum growth rate around -15^o C (Rogers and Yau, 1989, see Fig. 3.1).

Growth by accretion occurs when an ice particle overtakes or captures supercooled

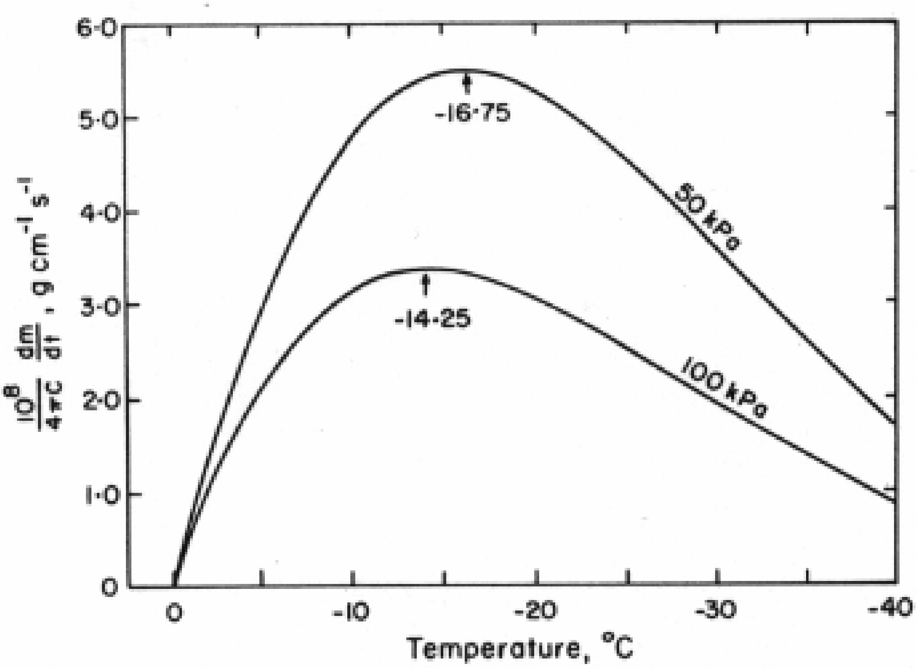

Figure 3.1: Normalized ice crystal growth rate by depostion as a function of temperature, for 50 kPa and 100 kPa. Adapted from Rogers and Yau (1989).

liquid droplets. This occurs mainly after the ice particle has grown to a sufficient size to begin to fall and collect the supercooled droplets. Hence, ice must initially grow by deposition at the top or mid-level of the cloud and only later by accretion as it falls through the cloud. Aggregation is the joining of multiple ice particles to form one large snowflake. This process generally occurs when temperatures are warmer than -10^oC, with the largest snowflakes occurring when the temperature is near 0^oC.

In this thesis, temperature is included at each level in an analysis of the ingredients in order to assess the likelihood of ice nucleation and to anticipate enhanced precipitation rates associated with rapid snowflake growth. The minimum cloud-top temperature component of the efficiency analysis is best performed using satellite-derived cloud-top temperature data and inspection of soundings during the event; however, forecast soundings and temperature on isobaric surfaces can provide an estimate of the likelihood that ice will be initiated in an event. Snowflake growth can be assessed in the IBM using model-predicted temperature by evaluating whether an area of strong forcing for ascent coincides with a region of maximum depositional growth ($T \approx -15^oC$). In this situation, heavy precipitation is possible provided sufficient moisture is present (Auer and White, 1982).

3.1.5 Temperature

An analysis of the temperature ingredient in a winter season mid-latitude cyclone addresses the precipitation type, or whether the precipitation will fall as rain, snow, ice pellets, or freezing rain[2]. The temperature ingredient is best diagnosed through the careful monitoring of observed temperature profiles as the storm develops; however, isobaric analyses of model-predicted temperature and moisture fields can help forecasters to anticipate precipitation type well in advance of the event. As with other forecasting rules of thumb, the conventional guidelines for predicting precipitation type are best applied in the context of a physical understanding of the thermodynamics governing precipitation type.

In a winter season weather system, precipitation is usually formed initially as snow and the thermal structure of the layer through which it falls determines the type of precipitation that will reach the ground. The initiation and growth of the original

[2] Freezing rain is defined as rain that falls in liquid form but freezes upon impact, and ice pellets (or sleet) are transparent or translucent pellets of ice, 5mm or less in diameter, which form from the freezing of rain drops or the refreezing of largely melted snowflakes when falling through a below-freezing layer of air near the earth's surface (Huschke, 1959).

ice crystals requires special consideration and was the subject of section 3.1.4, which focused on the efficiency ingredient. The discussion begins here with ice crystals that have grown large enough to fall from the cloud.

The amount of heat transferred to a melting ice crystal is proportional to (1) the difference between the temperature of the crystal (generally 0^{o}C) and the surrounding air, and (2) the amount of time the crystal spends at that temperature. Therefore, the ability of an ice crystal to melt depends on its fall velocity (related to its size and shape), crystal structure, and the temperature of the air through which it falls. If the air temperature remains below freezing between the level of ice crystal initiation and the ground, the precipitation will fall to the ground as snow. However, if a layer of warm (above freezing) air exists, either elevated or extending to the surface, there is the potential for one or more phase changes to occur before the precipitation reaches the ground.

Monotonically Decreasing Temperature Profile

For an atmospheric temperature profile which decreases monotonically with height, with an above-freezing layer extending to the surface, the precipitation will remain frozen and fall as snow if the wet bulb temperature is below 0^{o}C throughout the column. This is because ice (liquid) begins to sublimate (evaporate) if it falls through an unsaturated layer. The environmental temperature will cool due to this sublimation (evaporation) and the frost point (dew point) will rise, so that both approach the wet-bulb temperature. For the case of a surface warm layer wet-bulb temperature greater than 0^{o}C, there is the potential for partial or complete melting of the ice crystal. The probability that the precipitation will be snow has previously been expressed simply in terms of the depth of the warm layer (or, the height of the freezing level above ground). Table 3.4 presents the work of McNulty (1988) describing the likelihood as a function of warm layer depth that the precipitation type will be snow. Notice that the temperature of the warm layer is not considered here. McNulty (1988) also notes, "On the average,

Freezing Level	Chance of Snow
35 hPa or 290 m	50 %
25 hPa or 201 m	70 %
12 hPa or 96 m	90 %

Table 3.4: Relationship between the freezing level for a temperature profile decreasing monotonically with height and the likelihood that the precipitation type will be snow, adapted from McNulty (1988).

the freezing level must be at least 1200 feet above the surface to insure that the snow will melt to rain." This statement can be extended by recognizing that in the Western Plains regions of the United States, the 850 hPa surface is approximately 1200 feet above ground. Therefore, the 0^{o}C 850 hPa isotherm marks approximately the "rain edge" of the rain-snow boundary in these locations. Areas with an 850 hPa temperature greater than 0^{o}C are nearly certain to experience rain, however a close inspection of McNulty's statement reveals that it does not comment on the likelihood of precipitation falling as snow for temperatures less than 0 ^{o}C. Moreover, Table 3.4 shows that even for a freezing level at 96 m (or approximately 12 hPa) above ground, there is still a 10% chance that the precipitation will not be snow. Therefore, according to this interpretation of McNulty's work, the conventional use of the 850 hPa 0°C contour as the "rain-snow line" must be applied with caution, particularly in the "snow regime."

Temperature Profile with an Elevated Warm Layer

In the event of an elevated layer of above-freezing temperature with below-freezing temperatures underneath it (Fig. 3.2), the potential exists for freezing rain or sleet/ice pellets. The degree of melting that occurs in the warm layer is the key difference

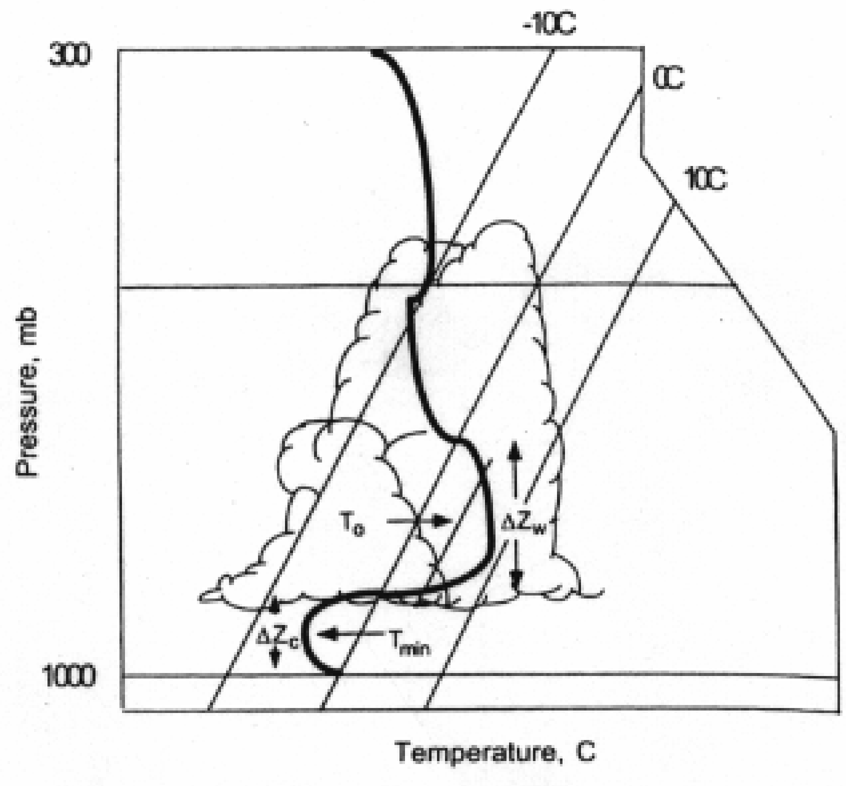

Figure 3.2: Schematic of an Elevated Warm Layer. Thick solid line is ambient air temperature, thin solid lines are -10 ^{o}C, 0 ^oC, and 10 ^{o}C isotherms. Adapted from Czys et al. (1996).

between conditions characteristic of freezing rain and those of sleet (Penn, 1957). If the snow completely melts to a liquid in the warm layer, then freezing rain or rain is likely. However, if the snow is only partially melted when it reaches the cold air beneath the warm layer, it begins to re-freeze immediately due to the presence of the remaining ice nuclei and falls to the ground as sleet or snow.

Czys et al. (1996) present a means of determining the degree of melting in an elevated warm layer based on the temperature of the elevated warm layer and the depth of that layer. The authors introduce a nondimensional parameter τ to assist in the determination of whether complete melting can be expected in an elevated warm layer and thus, in the diagnosis of freezing rain and ice pellets. In their study, τ is defined for a particle of a given radius as the ratio between the residence time (t_{res}) of the particle in the warm layer and the time required for complete melting (t_{melt}). t_{res} is based on the vertical distance the particle must fall (i. e., depth of the warm layer) and the velocity at which it falls. The relationship describing t_{melt} is derived through a balance between the rate of energy required to transform the solid to a liquid and the rate that the environment can supply the needed energy.

The resulting nondimensional parameter τ, can be used to determine the degree of melting in an elevated warm layer for a given maximum particle radius. For $\tau \geq 1$, conditions are characteristic of complete melting and freezing rain is favored. For $\tau < 1$, only partial melting of the largest particles is expected and precipitation will likely fall as ice pellets or snow. Figure 3.3 shows isopleths of the threshold value, $\tau = 1$, for a range of ice particle radii, warm layer depths, and mean warm layer temperatures. Based on 17 case studies in the Midwestern winter season of 1995-1996, Czys et al. (1996) found

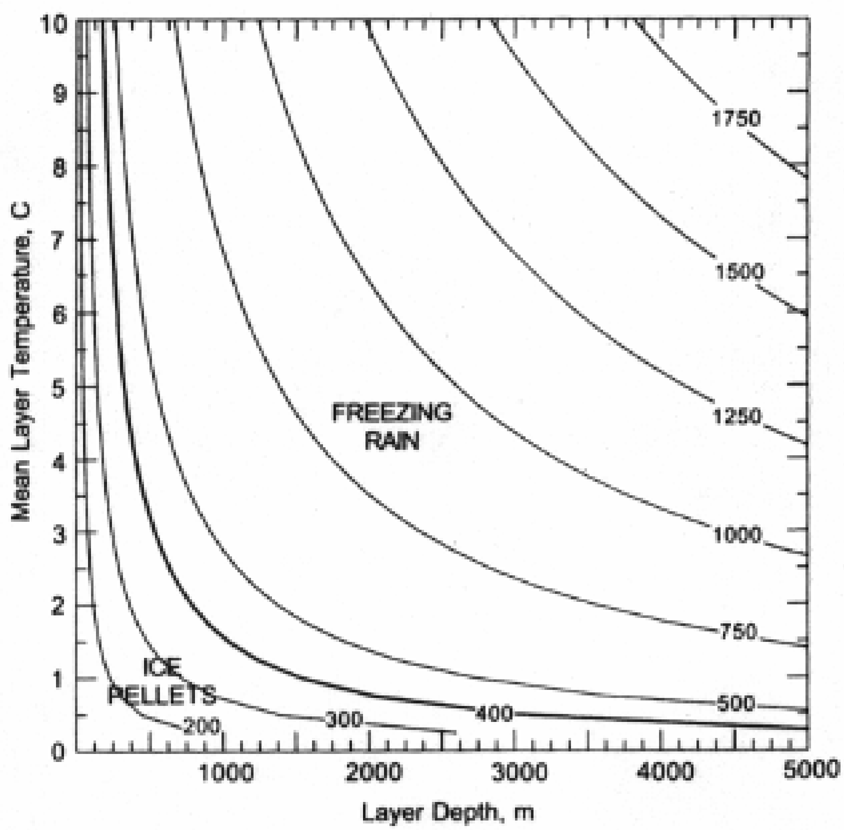

Figure 3.3: Isonomogram of $\tau = 1$ for different ice particle radii (μm) computed over a range of warm layer depths and mean temperatures. Adapted from Czys et al. (1996).

that a critical ice particle radius of $400 \mu m$ provides a reasonable level of accuracy. Thus, if the mean warm layer temperature and warm layer depth intersect in Fig. 3.3 above the $400 \mu m$ $\tau = 1$ isopleth, complete melting and freezing rain can be expected provided the surface temperature is below 0°C. If these parameters intersect below the $400 \mu m$ $\tau = 1$ isopleth, only partial melting is predicted.

An alternative to the Czys et al. (1996) technique considers only the warm layer maximum temperature. Because the depth of the warm layer is generally proportional to the maximum warm layer temperature, this simplification has proven to be a good diagnostic to determine the degree of melting (Baumgardt, 1999). Stewart and King

(1987) modeled the melting of snow as it falls through an elevated warm layer based on the empirical rates of snowflake melting described by Stewart (1985). The authors ran this model for various snowflake sizes, densities, maximum warm layer temperatures, and lapse rates. Evaporation and condensation were not considered, as the layer was assumed just saturated. Figure 3.4 presents these results and Table 3.5 summarizes the degree of melting as a function of maximum warm layer temperature. For the

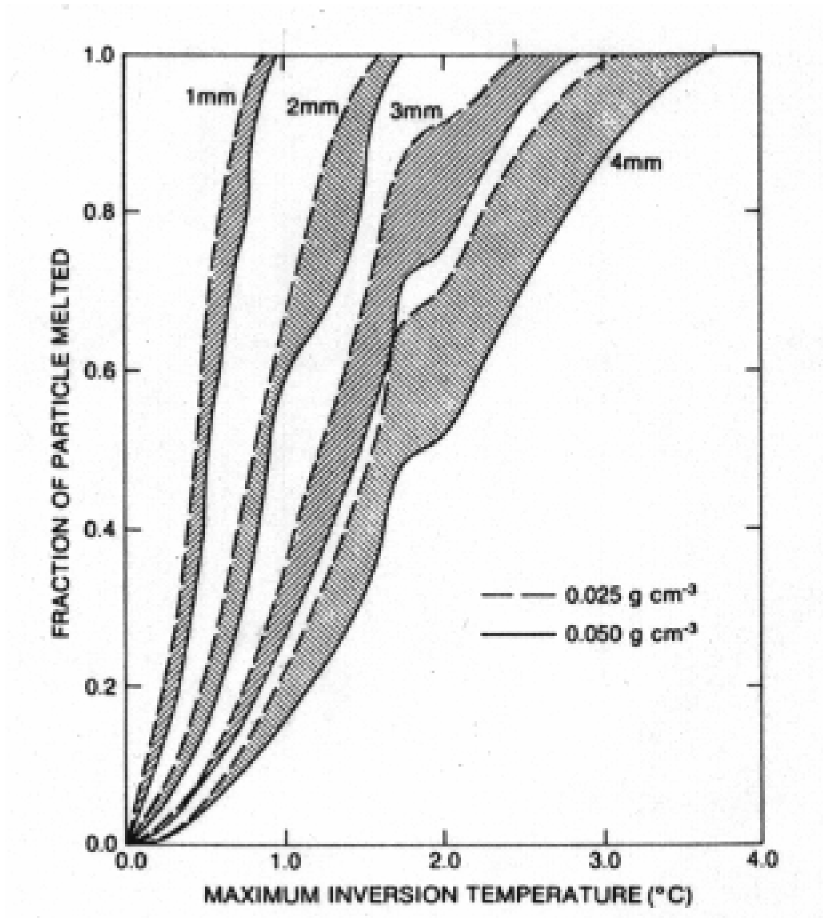

Figure 3.4: The degree of snowflake melting as a function of maximum warm layer temperature. The curves correspond to particle size expressed in terms of the raindrop-equivalent diameter, and for two different initial snowflake densities. Adapted from Stewart and King (1987).

case of complete melting (corresponding to a warm layer temperature $> 3-4^oC$), it is

Max. T of Warm Layer	Degree of Melting
$> 3 - 4^o$C	Melts Completely
$1 - 3^o$C	Partial Melting
$< 1^o$C	Very Little Melting with Re-freezing to Snow

Table 3.5: Summary of results from Stewart and King (1987), relating the degree of snowflake melting in an elevated warm layer to the maximum temperature of the warm layer.

also important to consider the temperature of the cold layer beneath the warm layer (McNulty, 1988). If the minimum temperature of the cold layer is greater than -10^o C, it is unlikely that the freezing process can be initiated so the precipitation will remain as a liquid until it reaches the ground. Provided the ground temperature is below freezing, this will result in freezing rain. When the minimum temperature of the cold layer is less than -10^o C, it is more likely that freezing will be initiated and snow or sleet will result provided there are enough ice nuclei. The depth of the cold air will determine the subsequent degree of re-freezing and, thus, whether the precipitation will be snow or sleet.

Summary

The precipitation type analyses described above are best performed with the use of modeled or observed soundings. Because observed sounding data is usually only available at 12-hour intervals, it may be useful to infer changes in the lower tropospheric thermal structure between balloon launches. Penn (1957) discussed the influences on the evolution of a temperature profile: thermal advection, adiabatic temperature change associated with vertical displacement, and non-adiabatic heating or cooling. Thermal advection by the horizontal wind is generally the dominant process, however this can act in opposition to an adiabatic temperature change. Because the horizontal advection of warm air is generally associated with upward vertical motion, warming associated with the advection can be reduced by adiabatic cooling associated with the rising air parcels. The net effect can be a reduction in the rate of warming by advection alone by roughly 50%. Additionally, diabatic processes can influence the temperature profile. Evaporational cooling when precipitation falls through a dry layer can reduce the temperature by 5-10^{o}C per hour until the air is saturated and the temperature reaches the wet bulb temperature. In very heavy snow events, the freezing level may also be altered by the absorption of latent heat when snow is melted to rain in a warm layer.

Figure 3.5 presents a summary of the steps involved in the diagnosis of precipitation type. This figure illustrates the complexity of the physical processes involved in determining precipitation type. Given forecasted and observed soundings, the ideas presented above will allow forecasters to perform a reasonable assessment of the likelihood that precipitation will be snow, ice pellets, freezing rain, or rain. However, in order to include a determination of precipitation type on isobaric surfaces with the other ingredients, the analysis is limited to diagnostics that can be computed at one level or layer in the atmosphere. Thus, in the ingredients maps, the 850 hPa 0^{o}C "rain-snow line" will be used as a rough guideline for a determining precipitation type. This guideline is only reliable when the forecast region is more than a few hundred kilometers to either

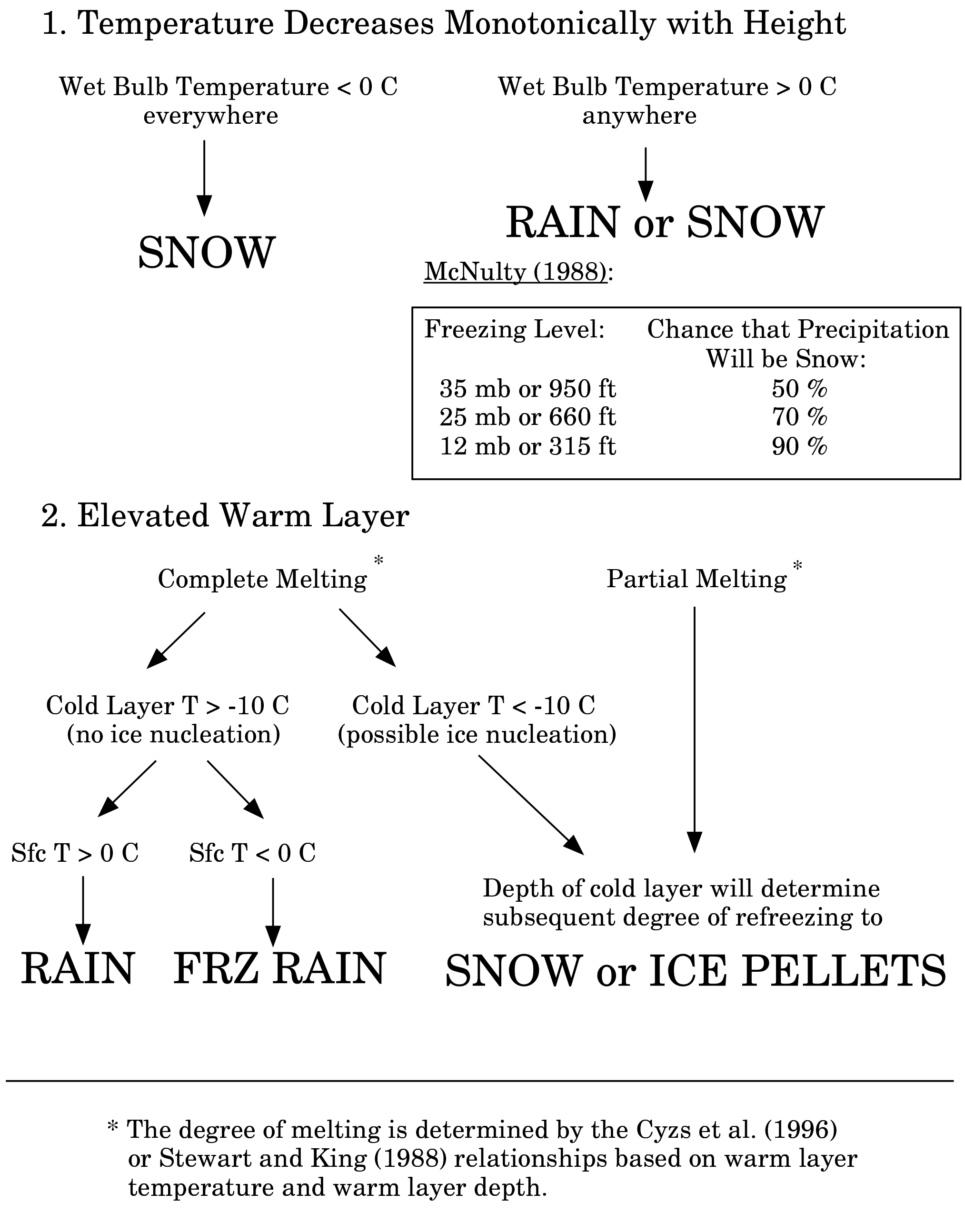

Figure 3.5: Summary of the steps involved in a diagnosis of precipitation type. See text for explanation.

side of the 0^{o}C isotherm and more than a few degrees cooler than 0^{o}C, and will be used in conjunction with an analysis of forecasted and observed soundings when the forecast area is any closer or any warmer.